Imaging Barriers to Diffusion by Pair Correlation Functions

Michelle A. Digman[†‡] and Enrico Gratton[†*]
[†]Laboratory for Fluorescence Dynamics, Department of Biomedical Engineering, and [‡]Optical Biology Core, Development Biology Center, University of California, Irvine, California

ABSTRACT Molecular diffusion and transport are fundamental processes in physical, chemical, biochemical, and biological systems. However, current approaches to measure molecular transport in cells and tissues based on perturbation methods such as fluorescence recovery after photobleaching are invasive, fluctuation correlation methods are local, and single-particle tracking requires the observation of isolated particles for relatively long periods of time. We propose to detect molecular transport by measuring the time cross-correlation of fluctuations at a pair of locations in the sample. When the points are farther apart than two times the size of the point spread function, the maximum of the correlation is proportional to the average time a molecule takes to move from a specific location to another. We demonstrate the method by simulations, using beads in solution, and by measuring the diffusion of molecules in cellular membranes. The spatial pair cross-correlation method detects barriers to diffusion and heterogeneity of diffusion because the time of the correlation maximum is delayed in the presence of diffusion barriers. This noninvasive, sensitive technique follows the same molecule over a large area, thereby producing a map of molecular flow. It does not require isolated molecules, and thus many molecules can be labeled at the same time and within the point spread function.

INTRODUCTION

Fluorescence correlation spectroscopy (FCS) has emerged as a very powerful method for studying the motions of proteins in both the interior and exterior of a cell. It provides information at the single-molecule level by averaging the behavior of many molecules, and thus yields very good statistics. Single-particle tracking (SPT) is also a highly sensitive technique for measuring particle movement. However, the FCS method suffers in terms of spatial resolution, and the SPT technique only allows for the tracking of isolated molecules. Here we propose a change of paradigm by introducing a method that uses the spatial pair cross-correlation function (pCF) to overcome this limitation. Our method measures the time a particle takes to go from one location to another by correlating the intensity fluctuations at specific points on a grid independently of how many particles are in the imaging field. Therefore, the average path of the particles can be traced. For example, our method can be used to detect when a protein passes the nuclear barrier and the location of the passage. This information cannot be obtained with the fluorescence recovery after photobleaching technique or any other image correlation spectroscopy method. Instead, our method builds on some recent work using dual-foci FCS (1) and bridges the two technologies (FCS and SPT) by providing single-molecule sensitivity in the presence of many molecules. We illustrate the potential of this new approach by examining a biological problem for which SPT has provided results that cannot be confirmed by traditional FCS measurements because of the lack of spatial resolution. Our method has much broader applicability for studies of membrane organization and dynamics because it works in three dimensions and can be applied to the interior of the cell.

The organization of natural membranes in microdomains with specific properties has been a matter of great debate during the last decade (2–5). Two models—the raft and the transient confinement zone—were recently proposed to describe this organization (2,6). Although it is known that cellular membranes are heterogeneous in terms of their chemical composition and physical properties, conjectures regarding the size and the lifetime of membrane microdomains remain controversial. There is general agreement that in biological membranes these microdomains are small and short-lived (7). If the domains are small, FCS cannot resolve regions of different diffusion, and SPT with very high spatial resolution requires statistics of many particles and could fail in showing transient regions of different mobility.

The method proposed here advances the field because it has the capability to grab both the spatial and temporal dimensions of microdomains on the proper scales and in live cells. Our method is based on cross-correlation functions computed at a pair of points at a given distance from each other. The time of the maximum of the correlation measures the average time the same molecule takes to migrate from one location to another in the membrane. This time is inversely proportional to the diffusion coefficient. This approach allows us to track the same fluorescent molecule in a sea of many other fluorescently labeled molecules in the lipid bilayer. If we systematically calculate the spatial pCF between any two points in the membrane, we can generate a map of molecular migration, as well as barriers to diffusion, over a large area.

In the transient confinement zone model of natural membranes, lipid molecules, as well as membrane proteins, stay confined in small zones of the membrane until they cross the barrier between the zones (6,8). In a given zone, the

Submitted February 9, 2009, and accepted for publication April 27, 2009.

*Correspondence: egratton22@yahoo.com

Editor: Elliot L. Elson.

0006-3495/09/07/0665/9 $2.00

doi: 10.1016/j.bpj.2009.04.048

diffusion and concentration of the lipid molecules do not differ from those in the neighboring zones. According to this model, the only difference between the presence and absence of a confinement zone is in the instantaneous flow of molecules throughout the boundaries of zones, which is different from the flow inside a zone. Zone barriers were originally detected with the use of SPT. In a series of elegant articles, Kusumi and co-workers (6,8) demonstrated that lipids attached to gold particles were transiently restricted to a small region of the membrane. They found that the size and height of the barriers between confinement zones are dependent on the type of cell and other biologically significant parameters. They detected zone boundaries using high-speed particle tracking and a sophisticated algorithm to analyze the particle trajectories that can detect local restriction to motion. If the organization of the membrane in transient confinement zones has important biological consequences, it will be desirable to have a different and general method to establish the map of the confinement zones.

Spatial pCF

The basic idea behind our method is to statistically follow the same fluorescent molecule as it diffuses in the membrane. Fig. 1 schematically shows the principle of the method. The fluorescence intensity is rapidly sampled (compared with the motion of the particle) at several points in a grid. As particles migrate, they appear at different points of the grid (Fig. 1, *left panel*). Only the same particle will produce an average cross-correlation with a given time delay at two different points in the grid. For example, a fluctuation in intensity at position 1 will statistically correlate with a fluctuation of the intensity at position 2 at a later time if the same particle is moving (with some delay) to position 2. Fluctuations at position 3 in the grid (the other side of the barrier in *blue*) will never correlate with the fluctuations at position 1 or 2. If we map the amount of correlation between pairs of points (1,2 and 2,3) we will see a discontinuity in the amount of correlation between points 2 and 3, but not between points 1,2 and 3,4. If instead of an impenetrable barrier, we have obstacles as shown in the right panel, we could observe the same particle on the other side of the obstacle but with a delayed correlation. If we cross-correlate the intensity fluctuations at each point of the grid, we produce a map of molecular flow with a resolution given by the size of the point spread function (PSF; shown in *light blue*), which is ~250 nm in the plane of the grid.

In the example of Fig. 1, we use two-dimensional (2D) diffusion, but the principle of the method is valid for diffusion in three dimensions. By detecting the same molecule at two different locations, we can measure the average time a molecule takes to move between those two locations. Since the measurement is exquisitely local to a pair of points, if there is a delay from the expected average time to diffuse the distance of the two points, we can make inferences about the existence of diffusion barriers between those two points. By repeating the calculation at several pairs of adjacent locations, we can trace the contour of the barrier, if it exists. One important consequence of the proposed pair-correlation method is that diffusion is measured by the average time particles (molecules) take to travel between two points. Since the position of the two points is arbitrary, the anisotropy of the motion can also be measured. This method is substantially different from the conventional FCS method, in which the duration of the intensity fluctuation is measured as the molecule transits across a focused laser beam.

The idea of measuring correlation between two separate points is not new. Traditionally, the two points are obtained by focusing two laser beams at a distance (fixed or variable). Using this approach, accurate measurements of diffusion coefficients can be achieved and the flow of molecules between the two points measured (1,9). However, the information obtained by this approach is local and is obtained one pair at a time. In our approach, we use only one laser beam that is moved rapidly at different locations in a repeated pattern (generally a line or a circle). The entire pattern is repeated in ~1 ms. We measure the correlation between every pair of points in the pattern. The result is a map of molecular flow and thus also a map of barriers to flow. Furthermore, our approach is applicable to conventional laser scanning

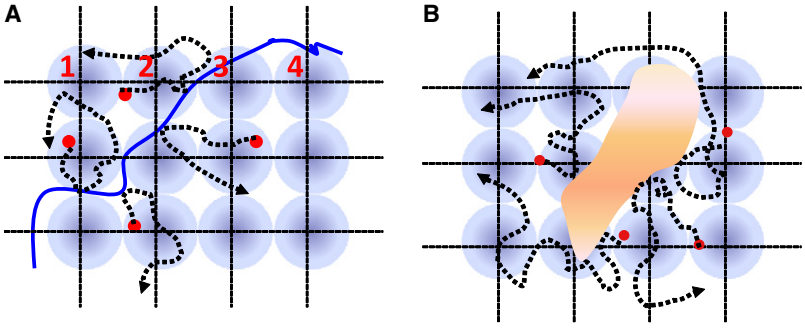

FIGURE 1 Schematic of the spatial pair-correlation method. The fluorescence intensity is rapidly sampled (compared with the motion of the particles) at several points in a grid (labeled 1, 2, 3, 4). As particles migrate, they appear at different points of the grid. Only the same particle will produce an average cross-correlation with a given time delay at two different points in the grid. For example, a fluctuation in intensity at position 1 will statistically correlate with a fluctuation of the intensity at position 2 if the same particle is moving (with some delay) to position 2. Fluctuations at position 3 in the grid (the other side of the barrier in *blue*) will never correlate with the fluctuations at position 1 or 2. If we map the amount of correlation between pairs of points (1,2 and 2,3), we see a discontinuity in the correlation between 2 and 3 but not between 1,2 and 3,4. If instead of an impenetrable barrier we have obstacles, as shown in the right panel, we could observe the same particle on the other side of the obstacle but with a delayed correlation. If we cross-correlate the intensity fluctuations at each point of the grid, we produce a map of molecular flow with a resolution given by the size of the PSF shown in light blue, which is ~250 nm in the plane of the grid.

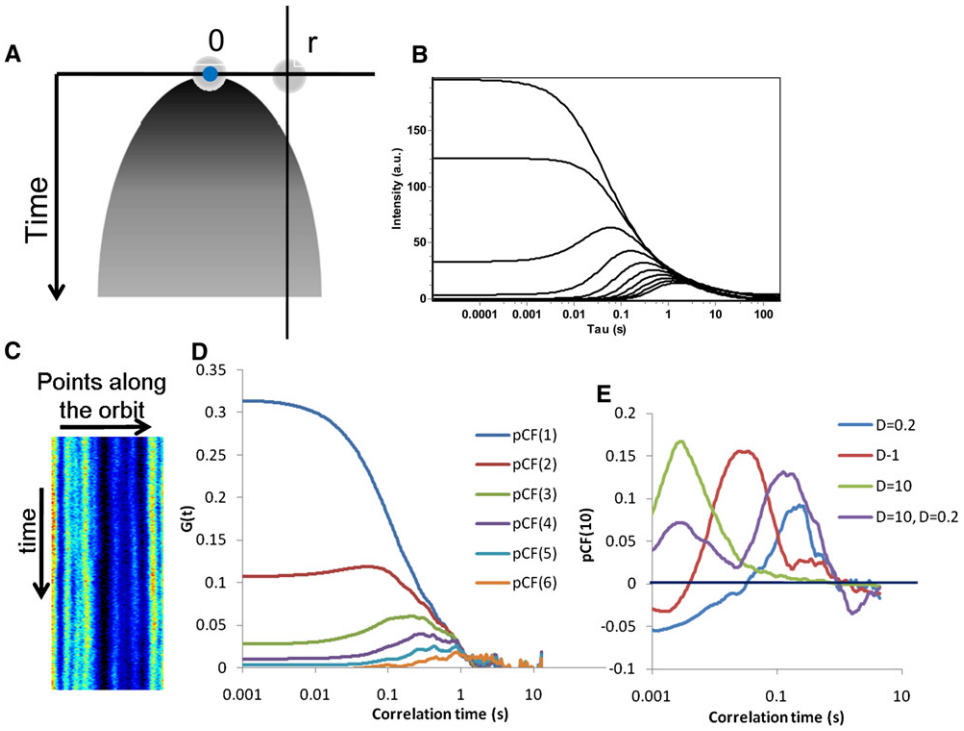

FIGURE 2 PCFs. (*A*) Particle observed at time $t = 0$ at the origin can be found at a distance r with a probability (shown schematically by the shaded parabolic shape) proportional to the fluorescence intensity at a given distance. (*B*) The fluorescence intensity is calculated at different distances from 0 to 2 μm in steps of 0.2 μm from the origin along a vertical line with respect to the plot in part *A*. For this calculation, the waist of the PSF was 0.3 μm and the diffusion coefficient $D = 1.0$ μm^2/s. (*C*) Intensity carpet for simulation of 500 particles diffusing on a plane with a diffusion coefficient of 0.1 μm^2/s shown in the color-coded image. The warmer colors correspond to higher intensities. (*D*) PCFs at different pixel distances from 1 to 6. The pCF at a distance of 6 pixels (0.9 μm) falls below zero. (*E*) pCF(10) calculated at a distance of 10 pixels for different values of the diffusion coefficient. The maximum of the pCF(10) function moves at longer times as the diffusion coefficient decreases. The amplitude of the correlation remains approximately constant. When two molecular species with different diffusion constants are present simultaneously, there are two maxima of the pCF due to the different time delays of the two species in reaching a given distance. At short correlation times, the pCF function can be negative, indicating spatial antibunching.

microscopes, which are readily available in most biology laboratories.

Fig. 2 schematically illustrates the expected intensity profile at two locations due to diffusion (Eq. 1) and the pair correlation concept. If a molecule at time $t = 0$ is at a given position shown by the blue dot (the size of the dot schematically indicates the size of the PSF), due to diffusion there is a probability of finding the molecule at any given distance from the original position, as shown in Fig. 2 *A* by the shaded parabolic area. Fig. 2 *B* shows the fluorescence intensity obtained at different times and distances from the origin as calculated using Eq. 2.

Description of the experimental setup: orbital scanning

In our experimental setup, we acquire data by rapidly moving a diffraction-limited laser beam focused on the surface of the membrane (10). The fluorescence intensity is sampled at a rate such that spatial locations along the orbit are oversampled with respect to the waist of the laser beam. For example, if the waist of the diffraction-limited spot is 200 nm (which is typical for a confocal microscope), as this spot moves on the plane of the membrane (in a linear or circular pattern), we sample the intensity approximately every 100 nm. The exact distance is not important provided that we can sample several times during the motion of the laser beam along a distance comparable to the beam waist. For example, in our setup we can scan on orbit in ~1 ms. If the intensity is sampled every 15.62 μs, we have 64 points per orbit in 1 ms. If the distance between successive points is 100 nm, we can collect points in a line that is ~6.4 μm long. This length scale is adequate for studying membrane spatial heterogeneity from ~200 nm to microns, and on a timescale from microseconds to several minutes or hours. The parameters used for this example are typical and their values could be adapted to different experimental situations.

Simulated data: isotropic diffusion

Fig. 2 *C* shows simulated data collected along an orbit ~10 μm long with a sampling rate of 15.62 μs/pixel. Data are presented under the form of a ''carpet'' in which the x-coordinate represents the positions along the orbit, and the vertical coordinate corresponds to successive orbits. Since the laser beam moves at constant velocity along the scan line, there is a direct relationship between the position of a point in the carpet representation and the time the intensity is acquired at that point. If we extract a column of the carpet, this column will correspond to the intensity fluctuations at that location. Along the orbit, points are sampled every 15.62 μs in our simulations and in our instrument. During this time, a molecule in the membrane will only diffuse a few nanometers (assuming a diffusion coefficient of 0.1 μm^2/s), and when the same position is sampled again after 1 ms, the particle will have moved ~20 nm on average. If we perform the pair

cross-correlation calculation of the fluctuations occurring at two points along the orbit, we can determine the average time taken to reach that distance. Fig. 2 *D* shows the pCF calculated between points at a distance of 1, 2, 3, 4, 5, and 6 pixels along the orbital scan for simulated data. When the distance between the two points is small, the points are in within the PSF, which produces a correlation of the intensity fluctuations in a very short time. As the distance increases, the amplitude of the pCF starts at very low (even negative) amplitude and then increases at a later time. In Fig. 2 *E* we show results of a simulation using particles with different diffusion coefficients and a combination of these particles. The figure shows the pCF at distance of 10 points along the orbit for three different diffusion coefficients ($D = 10{,}1$ and $0{,}2\ \mu m^2/s$) and for a sample containing particles diffusing at 10 and $0.2\ \mu m^2/s$. The average time at which the maximum of the correlation is reached increases as the diffusion coefficient decreases. The width of the time of passage distribution is relatively constant (in the log axis plot) and it is ~1 decade in time. We anticipate that if two molecular species differ in diffusion coefficient by more than a decade, they will appear as separate peaks in the pCF. The sample containing the two species that are separated by a factor of 50 in the diffusion coefficient are indeed well separated. We also show that the pCF can be negative at short times (Fig. 2 *E*). The characteristic anticorrelation at short times and increased correlation at longer times signifies that we are detecting the same molecule at a later time. This is the spatial equivalent of the ''time antibunching'' principle. At longer times we have a maximum in amplitude of the cross-correlation curve that is due to the average transit time (diffusive or not) between the two locations. At very long distances the cross-correlation function decreases because the particle has a smaller chance to be detected at one specific point along a circle surrounding the particle, as described above. In Fig. 2 *D* we show that the amplitude of the correlation decreases with distance, whereas Fig. 2 *E* shows that for the same distance, the amplitude of the correlation is independent of the diffusion coefficient. This is because we are measuring the same particle with a spot the size of the PSF at different distances. The ratio between the size of the spot and a hypothetical line surrounding the particle decreases linearly as we go farther away from the particle.

If we neglect bleaching (as discussed further below), the time-integrated probability of detecting the same molecule at any given distance from the origin will be independent of the diffusion constant and of the direction if the membrane is isotropic. In short, if we trace a hypothetical circle around a particle, the particle will cross this circle at some time. If we only measure a segment of this hypothetical circle, the probability that a particle will pass through that segment will depend on the ratio between the size of the segment and the length of the circle. If this region of observation is kept constant in size (for example the size of the PSF), as we go farther from the center of the circle, the probability that a particle will be detected in this small region will decrease linearly with distance. Instead, the average time at which the particle will be detected depends on the (square of the) distance, as shown in Fig. 2 *B*. This probability was previously evaluated by several authors (11,12). For example, a closed expression was obtained by Saxton and Jacobson (11) in the context of diffusion of molecules in membranes.

Detecting obstacles to diffusion and anisotropic diffusion

In the previous section we showed that the same particle can be detected at a given distance from the original starting point. If the membrane is isotropic, the average time to reach a given location is independent of the direction. We plot the values of the pCF and compare the position of the maximum of the function in the different directions. If there is a barrier to diffusion at any given location, the only way the particle can reach the other side of the barrier is to go around the obstacle or pass over the barrier. The maximum of the correlation will be found at a longer time than in the absence of a barrier. By mapping the time of the maximum of the pCF for every pair of points in the image, we can establish the size and location of the obstacles. If the barriers are transient, we should also be able to measure the movement and/or dissipation of the barriers, provided that their dynamics is much slower than the diffusion dynamics.

In this study we performed correlation measurements along an orbit rather than for every point in a plane. The obstacles are on the plane, but the measurement is performed only along one line. Although we cannot detect all obstacles to diffusion (only those along the line or close to the line are detected), we are able to establish the principle of the method and to interpret experiments performed on membranes. If we plot the pCF between two points at a given distance for every point along the line, we see a delay of the time of the maximum of the pCF if there is a barrier nearby, as shown in Fig. 1. Fig. 3 shows simulated data in which particles are confined to particular regions and an impenetrable barrier exists among these regions (shown by the *squares*). As the line of measurement crosses these barriers, the same particle cannot be found at the other side of the barrier. The barrier produces a delay of the time for maximum correlation (in this case, to infinity) since the barrier cannot be crossed. The pattern of the pCF shown in Fig. 3 projected on the image directly gives the location of the barriers along the orbit.

MATERIALS AND METHODS

Materials

Mouse embryonic fibroblast (MEF) cells were cultured in high-glucose Dulbecco's modified Eagle's medium supplemented with 10% fetal bovine serum and grown at 37°C at 5% CO_2. Cells were transiently transfected with GAP-EGFP (20 amino acid membrane targeting sequence from GAP-43 that contains two palmitoylated cysteine residues) using Lipofectamine 2000 (Invitrogen, Carlsbad, CA) according to the manufacturer's protocol. MEF cells were plated on imaging dishes coated with 3 μg/mL

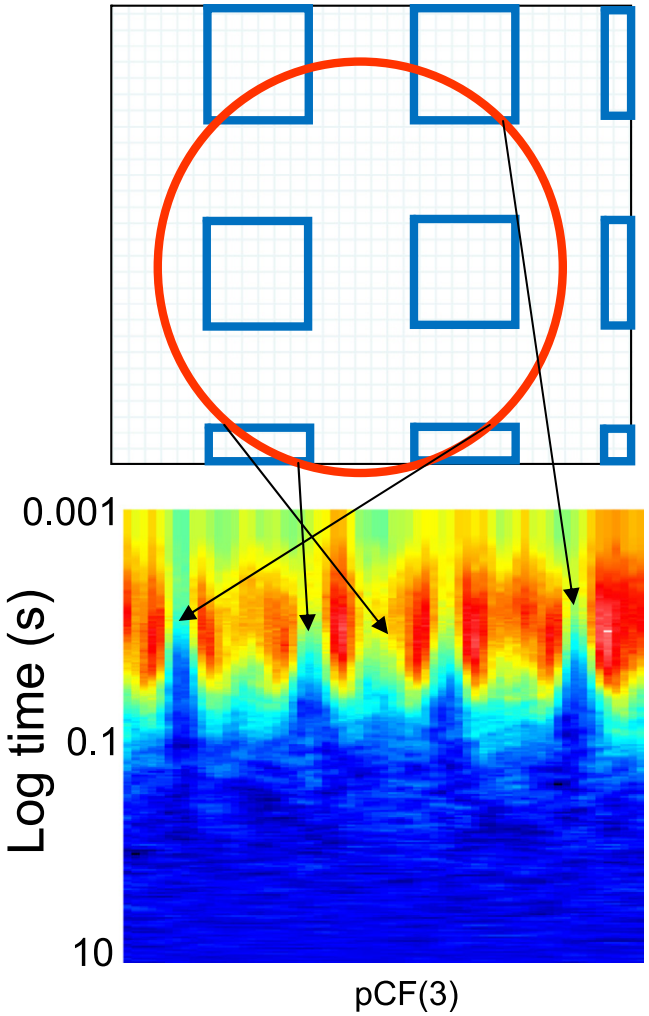

FIGURE 3 Simulation of particles diffusing in restricted zones of a membrane. The particles cannot cross the boundaries of the confinement zones shown in the upper part of the figure. Barriers to flow appear as "dark" vertical lines in the pCF carpet (no probability of finding a particle at a distance of 3 pixels along the orbit, pCF(3)). In this simulation the transient confinement zone size is 3.2 μm and the distance between zones is 12.8 μm. Transient confinement zones as small as 200 nm result in "visible" barriers to diffusion in the pCF representation.

fribronectin. For the DiO labeling, cells on imaging dishes were washed with phosphate-buffered saline and 2 mL of imaging media containing 1 μM DiO. Cells were incubated for 1–2 h before washing and imaging. All of the cells were imaged at room temperature.

Microscope

Microscopy measurements were performed with an in-house-built fluorescence microscope. For raster and circular scanning, the laser was guided into the microscope by x-y galvano-scanner mirrors (model 6350; Cambridge Technology, Cambridge, MA). The mirrors were driven in a preset scanning and synchronized with data. A photomultiplier tube (R4271; Hamamatsu Photonics, Bridgewater, NJ) was used for light detection in the photon counting mode. Data were acquired and processed by the SimFCS software developed at the Laboratory for Fluorescence Dynamics (University of California, Irvine, CA). A mode-locked titanium-sapphire laser with 80-fs pulses (Tsunami; Spectra-Physics, Palo Alto, CA) coupled to the back port of the microscope was used for excitation. A BG39 optical filter was placed before the photomultiplier for efficient suppression of reflected infrared used for excitation light. A 40× water immersion objective (Zeiss, Jena, Germany) with 1.2 N.A. was used for the measurements. The volume of the PSF was calibrated by measuring the autocorrelation curve for 20 nM fluorescein in 0.01 M NaOH, which was fit in turn with a diffusion coefficient of 300 $\mu m^2/s$. Typical values of w_0 (which define the PSF) were in the range of 0.30–0.50 μm depending on the laser wavelength and objective used. The average power at the sample was maintained at the milliwatt level.

Data analysis and data presentation

Simulations, data acquisition, and calculation of the pCF were done using the SimFCS software (Laboratory for Fluorescence Dynamics). The simulation part of the software was described previously. Documentation for the SimFCS software, which includes the simulation algorithms, can be found at http://www.lfd.uci.edu. Intensity data are presented using a carpet representation in which the x-coordinate corresponds to the point along the orbit (pixels) and the y-coordinate corresponds to the time. The autocorrelation function (ACF) and the pCFs at a given distance in pixels (pCF(pixel)) are displayed in pseudocolors in a image in which the x-coordinate corresponds to the point along the orbit and the vertical coordinate corresponds to the autocorrelation time in a log scale.

Derivation of the pCF for diffusing particles

The diffusion propagator is given by Eq. 1:

$$C(r,t) = \frac{1}{(4\pi Dt)^{3/2}} \exp\left(-\frac{r^2}{4Dt}\right), \quad (1)$$

where $C(r,t)$ can be interpreted as being proportional to the probability of finding a particle at position r and time t if the particle is at position 0 at time $t = 0$. The fluorescence intensity at any given time and position δr from the origin is given by

$$F(t,\delta r) = \kappa Q \int W(r)C(r + \delta r, t)dr, \quad (2)$$

where it is assumed that the fluorescence is proportional to the concentration, quantum yield Q, excitation-emission laser power, filter combination, and the position of the particle in the profile of illumination described by $W(r)$. The pCF for two points at a distance δr as a function of the delay time τ is calculated using the following expression:

$$G(\tau,\delta r) = \frac{\langle F(t,0) \cdot F(t+\tau,\delta r)\rangle}{\langle F(t,0)\rangle\langle F(t,\delta r)\rangle} - 1. \quad (3)$$

As in normal FCS, the pCF can be calculated analytically only for special cases of the profile of illumination function. For the simulations in this work, it was assumed that the illumination profile was described by a symmetric 2D Gaussian function.

We also note that the diffusion propagator described by Eq. 1 should be used with care. It is well known in the field of photon migration (13,14) that the propagator of Eq. 1 cannot properly describe diffusion at very short times since it violates the causality principle. For the simulations in this work, we used a Monte Carlo approach, which does not suffer from that limitation (15). Of course, the Monte Carlo approach does not give a closed form for the correlation functions.

RESULTS

Diffusion of beads in solution

Fig. 4 shows the carpet and the pCF analysis for a sample of beads freely diffusing in solution. The autocorrelation at each column gives the average diffusion coefficient. The maximum of the ACF is at time zero, since the particles

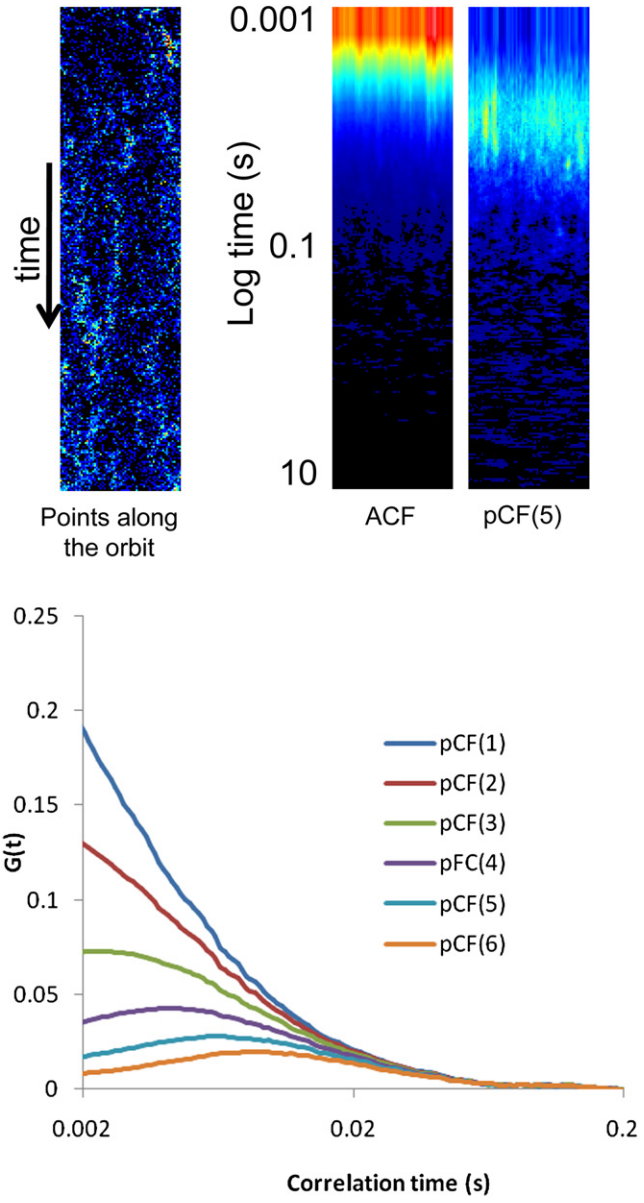

FIGURE 4 Beads in solution. The panels at left show the intensity carpet, autocorrelation (ACF, log time presentation) and the pair-correlation carpet calculated at a distance of 5 pixels along the orbit (pCF(5)). Along the orbit, 1 pixel corresponds to 0.15 μm. The plot shows the pCF calculated at a distance of 1–6 pixels.

correlate in the beam waist. If we correlate points along the columns that are at a distance of 1, 2, 3, 4, 5, and 6 pixels (1 pixel is 150 nm along the orbit), we can see that the time at which the maximum of the pair cross-correlation occurs increases as the distance increases, in accord with the prediction based on simulations.

Measurement of diffusion of DiO in the membrane of MEF cells

Fig. 5 *A* shows results obtained for the pCF along an orbit that is not crossing a specific cell boundary. The pCF follows the general pattern of free-diffusing particles except for one notable difference. At a location along the orbit that can be identified by a bright fluorescence ''feature'', there is an obstacle to the diffusion of the dye. At the long time, there is an increase in correlation in the region of the orbit at the bright feature, indicating that eventually the molecules will go around the obstacle (or through it). This result confirms our prediction that obstacles to diffusion are detected by the pCF approach.

Cell boundaries

As a positive control, we imaged two cells that were in close proximity, adjacent one to another and possibly in contact. We placed the scan orbit in a position that would cross both cells, as shown in Fig. 5 *B*. We expected that molecules would not pass through the physical boundary of the cell membrane, and that the pCF would indicate a lack of propagation of the molecules from one cell into another exactly at the membrane boundary. As shown in Fig. 5 *B*, the pCF shows obvious boundaries when the orbit crosses the boundaries between cells. We observed no crossing over this impenetrable barrier even at very long times.

Measurement at the basal membrane of MEF cells expressing GAP-EGFP

For the experiment using the GAP-EGFP protein in the membrane (Fig. 6 *A*), the pCF analysis shows that there are at least two diffusing molecular species. This is revealed by the broadening of the pCF at longer times, which indicates that there is more than one characteristic time for transporting protein molecules along the membrane (Fig. 6, *curves* at a distance of 8 and 16 pixels). The pattern of diffusion along the scan line is relatively uniform (Fig. 6, panel 0–120 s), indicating a lack of barriers to diffusion at specific locations. We note that the pCF was calculated by averaging measurements for ~120 s.

So far, our pCF analysis shows that in the GAP-EGFP system in MEF cells, there is no barrier for diffusion in the membrane except at locations with obvious macroscopic features (Fig. 4). However, we should limit our conclusions to the relatively long time of integration (120 s). If a barrier to diffusion exists for a shorter time, and this barrier moves on the membrane surface, we will have averaged out the position of the barrier. In other words, we could not have found a specific point along the orbit where particles were obstructed in their diffusive motion if this point moved with time. We systematically investigated shorter durations of the experiment by analyzing only a time segment of the overall experiment to look for short-lived obstacles. The signal/noise ratio decreased overall for short time traces because integration was shorter. However, if we compare the pCF obtained using the time trace from 0 s to 30 s within the overall time trace (0–120 s; Fig. 6), we see the appearance of what can be interpreted as transient barriers at one membrane location. Since

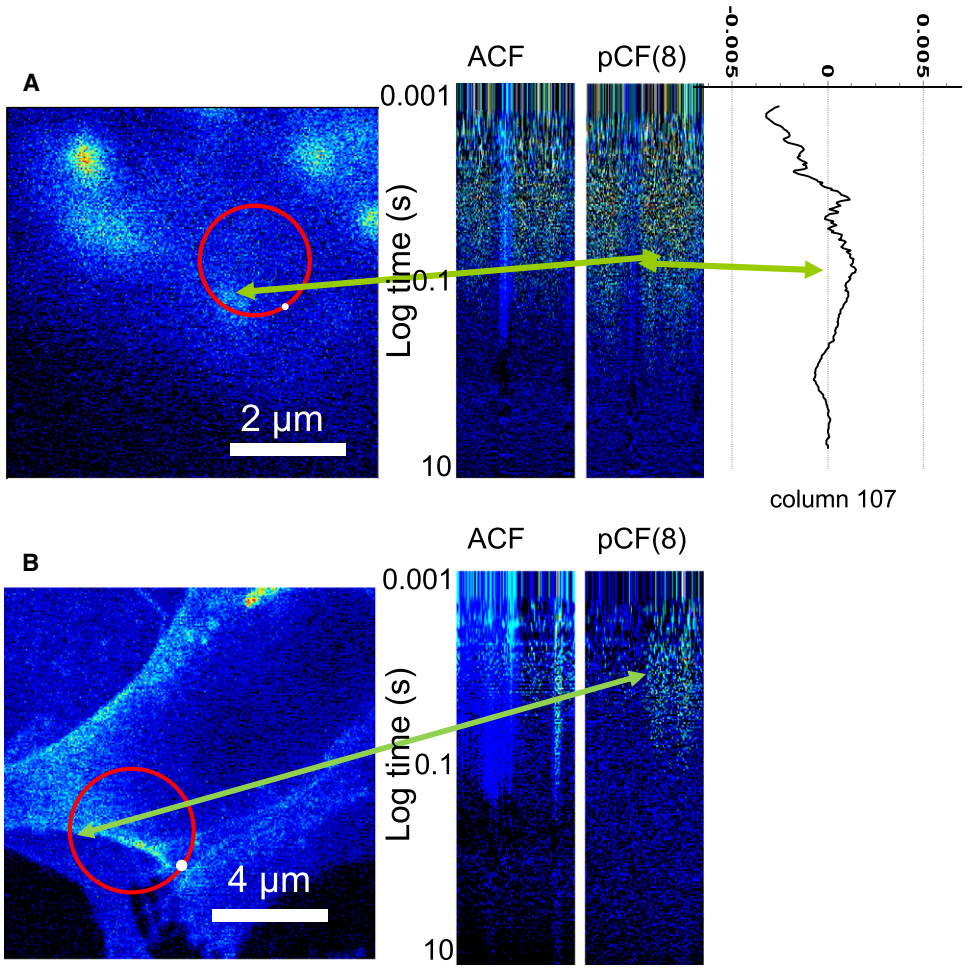

FIGURE 5 Detection of barriers to diffusion. (*A*) DiO in MEF cells. A barrier to diffusion is associated with a macroscopic "unknown" object in the membrane. The pCF(8) shows a discontinuity in the correlation at a given position along the orbit. The detail of the pCF at column 107 (out of 256 columns) along the orbit shows the molecules' delay in reaching a distance of 8 pixels (900 nm). (*B*) GAP-EGFP diffusing in two different cells. Obvious obstacles to diffusion are observed at the junction between cells. In this case, molecules never cross the cellular membrane barrier.

the signal/noise ratio is low, we cannot definitively prove the existence of this transient barrier; however, this approach appears to be promising enough to encourage further studies. In a different time segment (30–60 s), we could not discern any anisotropy in the diffusion (Fig. 6).

DISCUSSION

The pCF approach in FCS offers the potential to simultaneously track a large number of molecules. It does not require bright particles that are distinguishable from the background particles, and thus can provide a "true" measurement of the diffusion of single proteins in cells. In most SPT experiments, molecules are tagged with large, bright particles (e.g., gold or quantum dots) that can modify the overall transport dynamics of the protein. Of course, we need a fluorescent tag, but this tag could be a small fluorescent molecule. Tracking of individual molecules is averaged over regions of space. This massive tracking experiment can directly delineate obstacles to diffusion. Obstacles to diffusion can also be obtained by tracking individual particles, but at the expense of having to repeat the experiment many times, and having to rely on the selected particle to visit the region in which there is an anomaly in the diffusion behavior, and on specific algorithms to section the particle trajectory to determine the presence of obstacles by analysis. Instead, the pCF approach directly provides a map of the average behavior with very high time resolution (on the microsecond scale) and spatial resolution limited by diffraction. In this work we have shown the main features of our method, which can predict anticorrelation at short times for spatial separations larger than the beam waist, the decrease of the overall correlation as a function of distance due to the radial distribution of the particles, and the existence of a maximum of correlation at a distance corresponding to the average time necessary to reach a given position. We demonstrated the principle of the pCF approach using simulations and beads in solution. We then applied the pCF approach to the motion of the DiO dye on the membranes of live MEF cells. When we selected regions of the cell membrane that were free of obvious features, we found a relatively isotropic diffusion of the protein. However, when we used GAP-EGFP expressed in the inner membrane of the MEF cells, we found at least two components with different diffusion properties that could be identified by the appearance of two peaks in the pCF. It is interesting that we were

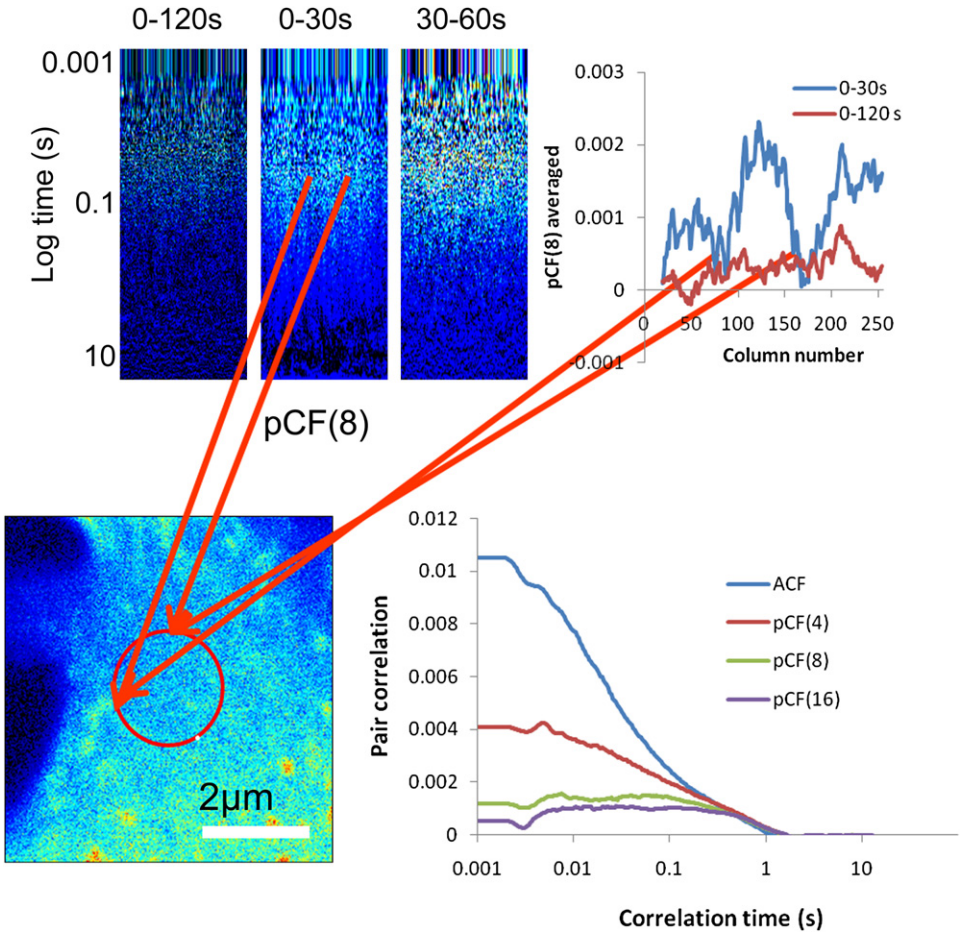

FIGURE 6 GAP-EGFP. Diffusing proteins are clearly visible in the ACF curve. The transport of molecules is uniform and isotropic at the basal membrane, although there are two or more diffusing components, as shown by the pair-correlation plot calculated at different distances of 8 and 16 pixels. The pCFs in the graph are averaged along the entire orbit. The pair-correlation operation was applied from 0 to 30 s and from 30 s to 60 s. In the first time segment, the correlation carpet is not uniform along the orbit (indicated by the *red arrow*), hinting at the existence of barriers to diffusion during the first time segment, but this obstacle to diffusion is not observed at later times (segment 30–60 s). The detail in the figure shows a projection of pCF(8) on the spatial axis. At specific locations the pCF seems to go to zero, indicating a barrier for diffusion, but in a different time segment of the same measurement the barrier appears to have dissipated.

able to distinguish at least two peaks, because this implies that there are two (or more) families of proteins diffusing in the membrane, and that the distribution of diffusion coefficients must be relatively bimodal (excluding the possibility that anomalous diffusion is responsible for this observation). Also, transient binding to relatively immobile features cannot explain this result unless the same molecule will preferentially bind to these features while other molecules will not. We observed a true heterogeneity of diffusion by observing fast- and slow-diffusing proteins that could be in clusters or interacting with other lipids for a relatively long period (seconds) of time.

We have shown internal controls for two situations. At the borders between cells, there is no flow of proteins between the cells, which is an obvious result. The pCF approach is exquisitely sensitive to macroscopic obstacles to diffusion if they exist. The other positive control was obtained by selecting an orbit that encompassed a relatively bright fluorescence structure of the cell. In this case we observed a barrier for diffusion, but the DiO molecules were found at the other side of the obstacle after some time delay.

We need to distinguish between ''average changes'' of fluorescence intensity that occur in a particular region of the membrane due, for example, to average changes in the concentration of the fluorescent molecules (lamellipodia extension is a typical example) and the correlation that originates from detecting the same molecule in two (or more) independent observation volumes. Generally, overall slow changes are easily identifiable. They give pCFs without a minimum at early times because the correlation extends over many pixels even at short times.

If bleaching occurs during the observation of the same molecule, of course the same particle cannot be measured any more. This is a common problem in SPT. However, bleaching only affects the overall signal/noise ratio (i.e., the amplitude of the pCF) without affecting the time a particle takes to travel a given distance. We note that in the line-scanning method, the same particle is not continuously illuminated, because it could meander in regions outside the line of measurement and statistically reappear at a given distance, thereby decreasing the probability of bleaching.

CONCLUSIONS

The pCF method is based on the spatiotemporal correlation of the position of the same particle at a given distance and a given time. The method builds on previous approaches based on the use of two foci in FCS and other image

correlation spectroscopy methods (1). In our approach, we have many independent foci (points along an orbit) that can be correlated simultaneously to measure the anisotropic diffusion of molecules. We show that obstacles to diffusion can be detected, and that the pCF algorithm can recognize and separate families of molecules that diffuse at different rates. For the GAP-EGFP protein in the membrane, we found that the diffusion is isotropic when averaged over a relatively long time (200 s), but transient barriers to diffusion could be present at shorter timescales.

This work was supported in part by the Cell Migration Consortium (grant U54 GM064346 to M.D. and E.G.) and the National Institutes of Health (grants P41-RRO3155 and P50-GM076516 to E.G.).

REFERENCES

1. Dertinger, T., A. Loman, B. Ewers, C. B. Muller, B. Kramer, et al. 2008. The optics and performance of dual-focus fluorescence correlation spectroscopy. *Opt. Express*. 16:14353–14368.
2. Brown, D. A., and E. London. 1998. Structure and origin of ordered lipid domains in biological membranes. *J. Membr. Biol.* 164:103–114.
3. Simson, R., B. Yang, S. E. Moore, P. Doherty, F. S. Walsh, et al. 1998. Structural mosaicism on the submicron scale in the plasma membrane. *Biophys. J.* 74:297–308.
4. Ishihara, A., and K. Jacobson. 1993. A closer look at how membrane proteins move. *Biophys. J.* 65:1754–1755.
5. Sheets, E. D., R. Simson, and K. Jacobson. 1995. New insights into membrane dynamics from the analysis of cell surface interactions by physical methods. *Curr. Opin. Cell Biol.* 7:707–714.
6. Kusumi, A., C. Nakada, K. Ritchie, K. Murase, K. Suzuki, et al. 2005. Paradigm shift of the plasma membrane concept from the two-dimensional continuum fluid to the partitioned fluid: high-speed single-molecule tracking of membrane molecules. *Annu. Rev. Biophys. Biomol. Struct.* 34:351–378.
7. Pike, L. J. 2006. Rafts defined: a report on the Keystone Symposium on Lipid Rafts and Cell Function. *J. Lipid Res.* 47:1597–1598.
8. Ritchie, K., R. Iino, T. Fujiwara, K. Murase, and A. Kusumi. 2003. The fence and picket structure of the plasma membrane of live cells as revealed by single molecule techniques. *Mol. Membr. Biol.* 20:13–18 [Review].
9. Korlann, Y., T. Dertinger, X. Michalet, S. Weiss, and J. Enderlein. 2008. Measuring diffusion with polarization-modulation dual-focus fluorescence correlation spectroscopy. *Opt. Express*. 16:14609–14616.
10. Ruan, Q., Y. Chen, E. Gratton, M. Glaser, and W. W. Mantulin. 2002. Cellular characterization of adenylate kinase and its isoform: two-photon excitation fluorescence imaging and fluorescence correlation spectroscopy. *Biophys. J.* 83:3177–3187.
11. Saxton, M. J., and K. Jacobson. 1997. Single-particle tracking: applications to membrane dynamics. *Annu. Rev. Biophys. Biomol. Struct.* 26:373–399.
12. Schmidt, T., G. J. Schutz, W. Baumgartner, H. J. Gruber, and H. Schindler. 1996. Imaging of single molecule diffusion. *Proc. Natl. Acad. Sci. USA*. 93:2926–2929.
13. Fishkin, J. B., S. Fantini, M. J. vandeVen, and E. Gratton. 1996. Gigahertz photon density waves in a turbid medium: theory and experiments. *Phys. Rev. E Stat. Phys. Plasmas Fluids Relat. Interdiscip. Topics*. 53:2307–2319.
14. Fishkin, J. B., and E. Gratton. 1993. Propagation of photon-density waves in strongly scattering media containing an absorbing semi-infinite plane bounded by a straight edge. *J. Opt. Soc. Am. A*. 10:127–140.
15. Ma, G., J. F. Delorme, P. Gallant, and D. A. Boas. 2007. Comparison of simplified Monte Carlo simulation and diffusion approximation for the fluorescence signal from phantoms with typical mouse tissue optical properties. *Appl. Opt.* 46:1686–1692.